Proceedings of IMECE '02
2002 International Mechanical Engineering Congress and Exhibition
November 17-22, 2002, New Orleans, LA

IMECE2002-33084

QUASI-STEADY STATE NATURAL CONVECTION IN LASER CHEMICAL VAPOR DEPOSITION WITH A MOVING LASER BEAM

Yuwen Zhang
Department of Mechanical Engineering
New Mexico State University
Las Cruces, NM 88003
E-mail: yuwzhang@nmsu.edu

ABSTRACT

Numerical analysis of laser chemical vapor deposition (LCVD) of Titanium Nitride by a moving laser beam is investigated numerically. The effect of natural convection due to temperature and concentration differences in the gases mixture is modeled and implemented into the thermal model of LCVD by a moving laser beam. The problem is formulated in the coordinate system that moves with the laser beam. The results show that the effect of natural convection on the shape of deposited film is very insignificant for cases with lower laser power but it becomes important when the laser power is increased.

NOMENCLATURE

C	concentration (kg/m³)
c_p	specific heat (J/kgK)
D	mass diffussivity (m²/s)
E	activation energy (kJ/mol)
h	thickness of the substrate (m)
k	thermal conductivity (W/mK)
K_0'	Arrhenius constant
M	molecular weight (g/mol)
m	mass flux (kg/m²)
P	laser power (W)
p	pressure (Pa)
q″	heat flux (W/m²)
r_o	radius of the laser beam (m)
R_u	universal gas constant (=8.314kJ/kmol)
S	source term in the energy equation
S_c	source term in the mass transfer equation
t	time (s)
T	temperature (K)
u	velocity component in x direction (m/s)
v	velocity component in y direction (m/s)
w	velocity component in z direction (m/s)
x	coordinate in length direction(m)
y	coordinate in width direction (m)
z	coordinate in height direction (m)

Greek Symbols

α	diffusivity (m²/s)
α_a	absorptivity
β	coefficients of thermal expansion (1/K)
β_c	concentration expansion coefficients (m³/kg)
γ	sticking coefficient
δ	thickness of the deposited film (m)
ΔH_R	heat of chemical reaction (J/kg)
ε	emissivity
ρ	density (kg/m³)

Subscripts

g	gas
i	initial value
s	substrate
∞	infinite

INTRODUCTION

Solid Freeform Fabrication (SFF) is an emerging manufacturing technology that directly creates three-dimensional parts from a CAD design [1,2]. The CAD data is transferred to a STL computer file, which is then sliced to generate two-dimensional sections of the virtual product. The physical product is built by layering two-dimensional sections of finite thickness. An extremely wide array of SFF technologies has been proposed for purposes of providing physical three-dimensional renderings of CAD data. However, only a few have been extended to build structurally-sound parts

of near full density. Almost always, the SFF technologies that fit into the latter group are powered by thermal fabrication of three-dimensional objects from powders or gases. To produce fully functional structural components, gases based approaches to SFF (such as Selective Area Laser Deposition; SALD), seems to be very promising [3-5]. It utilizes Laser Chemical Vapor Deposition (LCVD) technique, which can be based on reactions initiated pyrolytically, photolytically or a combination of both [2], to deposit the film at the desired location on the substrate. LCVD can also find its application on thin film coating and semi-conductor industry.

A very detailed literature review about Chemical Vapor Deposition (CVD) was given by Mahajan [6]. The difference between the LCVD and the regular CVD is that only a very small spot on the substrate is heated by the laser beam and vapor deposition occurs only on the heated spot in the LCVD process. Mazumder and Kar [7] reviewed the theoretical and experimental works about LCVD up to 1995. Jacquot et al. [8] proposed a thermal model of the SALD process using acetylene (C_2H_2) as the source gas. Various phenomena, which include heat conduction in the substrate, chemical reaction during carbon deposit, and mass diffusion of acetylene in the chamber are taken into account. The effect of chemical reaction heat on the heat conduction of the substrate was also taken into account. The temperature of the gases was, however, assumed to be uniform and therefore the heat transfer in the gas phase is neglected. Zhang and Faghri [9] developed a very detailed model of SALD process, which includes the submodels of heat transfer, chemical reaction and mass transfer, and the model was employed to simulate the laser chemical vapor deposition of TiN film on a finite slab with stationary and moving laser beams. The results showed that the effect of chemical reaction heat on the shape of deposited film was negligible.

The spot on the substrate under laser irradiation is at a very high temperature. The temperature difference in the source gases will cause natural convection in the chamber. The concentration of the gas mixture near the hot spot on the substrate is affected by the chemical reaction that takes place on the substrate. The concentration difference in the chamber becomes another driving force of natural convection in the chamber. For the cases of the LCVD by a stationary laser beam, Lee et al. [10] concluded that the effect of natural convection of the gas on the thin film deposition rate was negligible and the heat and mass transfer in the gases were dominated by diffusion. In the SALD process, the laser beam scans the substrate and the product of the chemical reaction forms a line on the top of the substrate. These lines, formed by multiple laser scans, are subsequently interwoven to form a layer part. In order to thoroughly understand the effects of various physical phenomena, including natural convection, on the SALD process, the LCVD with natural convection by a moving laser beam will be investigated in this paper.

PHYSICAL MODEL

The physical model of LCVD under consideration is illustrated in Fig. 1. A substrate made of Incoloy 800 with a thickness of h is located in the bottom of a chamber. Before the vapor deposition is started, the chamber is evacuated and then fills with mixture of H_2, N_2, and $TiCl_4$. A laser beam moves along the surface of the substrate with a constant velocity, u_b. The initial temperature of the substrate, T_i, is below the chemical reaction temperature. The vapor deposition starts after the surface temperature reaches the chemical reaction temperature. The chemical reaction that takes place on the top substrate surface absorbs part of the laser energy and consumes the $TiCl_4$ near the substrate surface. A concentration difference is therefore established and becomes the driving force of mass transfer. The physical model of the SALD process will include: natural convection, heat transfer in the substrate and gases, chemical reaction, as well as mass transfer in the gases.

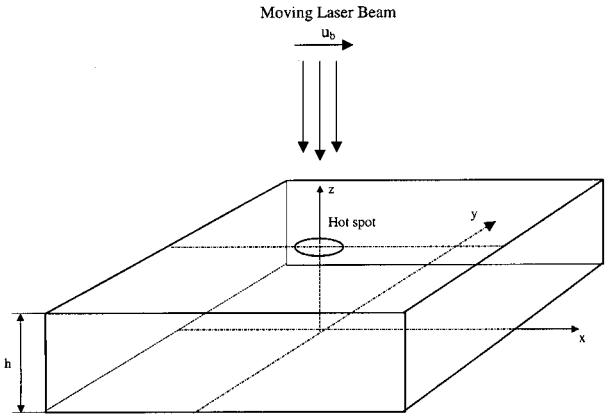

Fig. 1 Physical model of Laser Chemical Vapor Deposition

The laser beam travels with a constant velocity, u_b, along the surface of the substrate, which is a typical moving heat source problem [11]. If the substrate is sufficiently large compared with the diameter of the laser beam, which has an order of magnitude of 10^{-3}, a quasi-steady state occurs. The system appears to be in steady state from the stand point of the observer located in and traveling with the laser beam. By solving the LCVD with a moving laser beam in the moving coordinate system, the computational time will be substantiality saved, which will make numerical simulation to a significant number of cases possible.

Since the temperature of the substrate undergoes a significant change under laser irradiation, the constant thermal properties assumption does not apply [8-10]. Heat transfer in the substrate and gases is modeled as one problem with thermal properties reflecting the differences in each region. In the substrate region, the velocity will be set to zero in the numerical solution. The advantage of modeling the heat and mass transfer problem in the substrate and the gases as one problem is that the temperature distribution in substrate and gases can be obtained

by solving one equation, and the iteration procedure to match the boundary condition at substrate-gases interface can therefore be eliminated. Since the problem is symmetric about the xz plane, only half of the problem needs to be investigated. For a coordinate system moves with the laser beam as shown in Fig. 1, the laser beam is stationary but the substrate and the chamber move with a velocity $-u_b$. The heat and mass transfer in the substrate and gases are modeled with the following equations:

$$\frac{\partial \rho u}{\partial x}+\frac{\partial \rho v}{\partial y}+\frac{\partial \rho w}{\partial z}=0 \tag{1}$$

$$u\frac{\partial u}{\partial x}+v\frac{\partial u}{\partial y}+w\frac{\partial u}{\partial z}=-\frac{1}{\rho}\frac{\partial p}{\partial x}+\nu\left(\frac{\partial^2 u}{\partial x^2}+\frac{\partial^2 u}{\partial y^2}+\frac{\partial^2 u}{\partial z^2}\right) \tag{2}$$

$$u\frac{\partial v}{\partial x}+v\frac{\partial v}{\partial y}+w\frac{\partial v}{\partial z}=-\frac{1}{\rho}\frac{\partial p}{\partial y}+\nu\left(\frac{\partial^2 v}{\partial x^2}+\frac{\partial^2 v}{\partial y^2}+\frac{\partial^2 v}{\partial z^2}\right) \tag{3}$$

$$u\frac{\partial w}{\partial x}+v\frac{\partial w}{\partial y}+w\frac{\partial w}{\partial z}=-\frac{1}{\rho}\frac{\partial p}{\partial z}+\nu\left(\frac{\partial^2 w}{\partial x^2}+\frac{\partial^2 w}{\partial y^2}+\frac{\partial^2 w}{\partial z^2}\right)-g\beta(T-T_\infty)-g\beta_c(C-C_\infty) \tag{4}$$

$$\rho\left(\frac{\partial(uc_pT)}{\partial x}+\frac{\partial(vc_pT)}{\partial y}+\frac{\partial(wc_pT)}{\partial z}\right)=\frac{\partial}{\partial x}\left(k\frac{\partial T}{\partial x}\right)+\frac{\partial}{\partial y}\left(k\frac{\partial T}{\partial y}\right)+\frac{\partial}{\partial z}\left(k\frac{\partial T}{\partial z}\right)+S \tag{5}$$

$$\frac{\partial(uC)}{\partial x}+\frac{\partial(vC)}{\partial y}+\frac{\partial(wC)}{\partial z}=D\left(\frac{\partial^2 C}{\partial^2 x}+\frac{\partial^2 C}{\partial^2 y}+\frac{\partial^2 C}{\partial^2 z}\right)+S_c \tag{6}$$

where β and β_c are respectively the coefficients of thermal expansion and concentration expansion coefficient, respectively.

For the substrate region, the thermal properties are that of the substrate material, Incoloy 800. For the gases region, the thermal properties are determined by the individual thermal properties of H_2, N_2, and $TiCl_4$ as well as their molar fractions [12]. The mass diffussivity of $TiCl_4$ in the gas mixture is determined by Stefan-Maxwell equation [12] using the binary diffusivity of $TiCl_4$ with respect to each other species, which is calculated using the hard sphere model [12].

The source term in eq. (5) deals with the effects of laser beam heating and chemical reaction. The source term will be zero everywhere except at the substrate-gases interface under the laser spot. The heat flux at the substrate surface due to laser beam irradiation and chemical reaction is expressed as

$$q''=\frac{2P\alpha_a}{\pi r_0^2}\exp\left[-\frac{2(x^2+y^2)}{r_0^2}\right]-\varepsilon\sigma(T^4-T_\infty^4)-\rho_{TIN}\Delta H_R\frac{d\delta}{dt},\quad z=h \tag{7}$$

where $d\delta/dt$ is the deposit rate, which is expressed as [9]

$$\frac{d\delta}{dt}=\frac{\dot{m}}{\rho_{TIN}}=\frac{K_0}{\rho_{TIN}}\exp\left(-\frac{E}{R_uT_s}\right)C_s \tag{8}$$

where C_s represents the concentration of $TiCl_4$ at the surface of the substrate. The constant, K_0, in eq. (8) is defined as

$$K_0=(C_{H_2})_i(C_{N_2})_i^{1/2}K_0' \tag{8a}$$

The LCVD problem under investigation is steady state in the moving coordinate system and therefore, the deposition depth, δ, is not a function of time. The scanning time is translated into the spatial variable x by

$$\frac{dx}{dt}=-u_b \tag{9}$$

Substituting eq. (9) into eq. (8), an equation about the profile of the deposited film can be obtained.

$$\frac{d\delta}{dx}=-\frac{K_0}{u_b\rho_{TIN}}\exp\left(-\frac{E}{R_uT_s}\right)C_s \tag{10}$$

In order to use eq. (7) to determine the source term in eq. (5), the heat flux is treated as an internal heat source in the grid near the surface of the substrate, i.e.

$$S=\frac{q''\Delta x\Delta y}{\Delta V}=\frac{q''}{\Delta Z} \tag{11}$$

where $\Delta x,\Delta y,\Delta z$ represent the dimension of the control volume cell in the substrate near its surface.

The effect of the chemical reaction on the mass transfer is accounted for by a source term in eq. (6). The mass flux rate of $TiCl_4$ at the substrate is expressed as

$$\dot{m}_{TiCl_4}=\rho_{TIN}\frac{d\delta}{dt}\frac{M_{TiCl_4}}{M_{TiN}} \tag{12}$$

The source term in eq. (6) is then expressed as

$$S_c=-\frac{\dot{m}_{TiCl_4}\Delta x\Delta y}{\Delta V}=\frac{M_{TiCl_4}}{M_{TiN}}\frac{K_0}{\Delta z}\exp\left(-\frac{E}{R_uT_s}\right)C_s,\quad z=h \tag{13}$$

The boundary conditions of the velocities are

$$u=-u_b,\quad v=w=0,\quad |x|\to\infty \tag{14a}$$

$$v=\frac{\partial u}{\partial y}=\frac{\partial w}{\partial y}=0,\quad y=0 \tag{14b}$$

$$u=-u_b,\quad v=w=0,\quad y\to\infty \tag{14c}$$

$$u=-u_b,\quad v=w=0,\quad z=0,\infty \tag{14d}$$

The boundary conditions of eq. (5-6) are

$$T=T_i,\quad C=C_i\quad |x|\to\infty \tag{15a}$$

$$\frac{\partial T}{\partial y}=\frac{\partial C}{\partial y}=0,\quad y=0 \tag{15b}$$

$$T=T_i,\quad C=C_i\quad y\to\infty \tag{15c}$$

$$\frac{\partial T}{\partial z}=0,\quad C=0,\quad z=0 \tag{15d}$$

$$\frac{\partial T}{\partial z}=\frac{\partial C}{\partial z}=0,\quad z\to\infty \tag{15e}$$

NUMERICAL SOLUTION

The problem under investigation is a conjugated natural convection problem driving by temperature and concentration differences. The governing equations are discretized using the finite volume method [13]. The SIMPLEC algorithm [14] was employed to handle the linkage between velocity and pressure. The staggered grid was used to discretize solution domain. The pressure, temperature, concentration, and all properties are stored on the main grid, which is at the center of the control volume. The velocity components are calculated at the points that lie on the faces of the control volumes. The convection-diffusion terms in the momentum, energy and concentration equations are discretized by an exponential scheme. The resulted discrete equations are solved by using ADI (Alternative Directional Implicit) method. The underrelaxation factor for the velocity components is 0.5. Underrelaxation for pressure is not needed because SIMPLEC algorithm is employed.

The governing equations are written for the entire domain that includes both substrate and the gases. The velocity and concentration in the substrate region should be zero. The algebraic equations resulted from the control volume approach have the following format

$$a_P = \sum a_{nb}\phi_{nb} + b \qquad (16)$$

By setting $a_p=10^{30}$ in eq. (16) at the grid point located in the substrate region for momentum equations and mass transfer equation, the zero velocity and concentrate field can be achieved [15]. In order to ensure that the velocity field is not altered by the pressure correction, the pressure correction at the points in the substrate region must be zero. The above technique is also applied to achieve the zero pressure correction. The coefficients of the algebraic equations are altered before the algebraic equations are solved. The overall solution procedure is similar to that outlined in [9] and will not be repeated here. The typical number of iteration to get the converged solution is about 6000. In order to accelerate convergence, the initial temperature and concentration distributions for a specific case can be set as the converged temperature distribution for a similar case, which resulted in a reduction of the iteration number by 50%.

In order to simulate the LCVD in the moving coordinate system, the computational domain in x and y direction must be large enough so that the effect of the computational domain on the temperature and concentration distributions can be eliminated. The calculations were carried out for a non-uniform grid of 82 nodes in the x direction, 42 nodes in the y direction, and 82 node in the Z direction. Finer grid sizes and smaller false time steps were also used in the calculations, but their results did not provide a noticeable difference with the present grid size.

RESULTS AND DISCUSSION

In order to verify the validity of the code, the calculation is initially made with conduction in the substrate with moving laser beam. The conduction problem in the substrate is achieved by setting the thermal conductivity of the gas as zero so that there is no heat conduction in the vapor phase. The steady state surface temperature obtained by numerical solution is compared with the temperature distribution caused by a moving point heat source. The temperature expression of a semi-infinite body with a moving point heat source is [16]

$$T_s - T_i = \frac{P\alpha_a}{2\pi kr}\exp\left[-\frac{u(r+x)}{2\alpha}\right] \qquad (17)$$

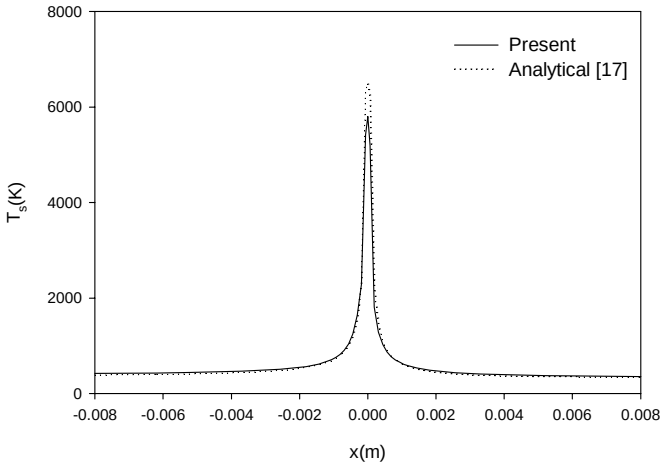

Fig. 2 Comparison between analytical and numerical solutions for pure conduction

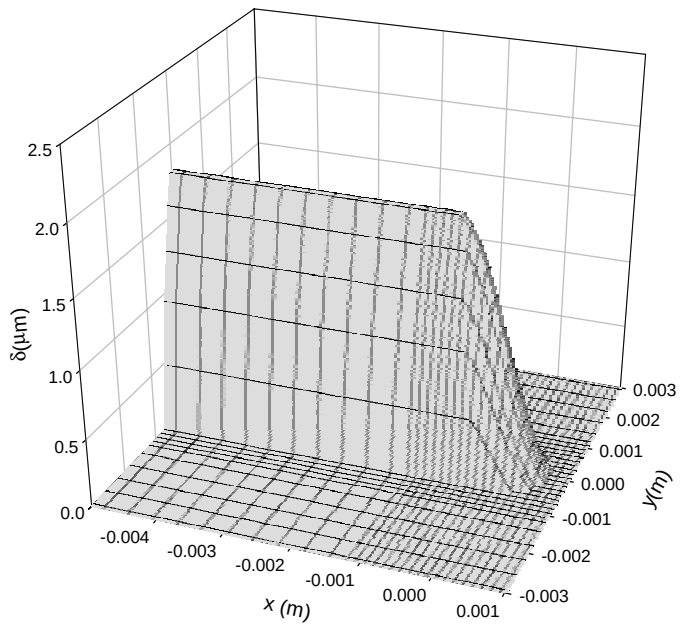

Fig. 3 Shape of the deposited film (P=300W, u_b=1.2mm/s)

In order to simulate conduction in the substrate subject to a moving point heat source, the heat flux at the substrate surface due to laser beam irradiation is expressed as

$$q''=\begin{cases}\dfrac{P\alpha_a}{\pi r_0^2} & r\le r_0,\quad z=h\\ 0 & r>r_0\end{cases} \tag{18}$$

where the moving heat source is assumed to be top-hat (uniform distribution) instead of Gaussian distribution because the latter results in the energy spread in a large spot. Effects of surface radiation and chemical reaction on the surface heat flux are also neglected in eq. (17) in order to simulate pure conduction in the substrate.

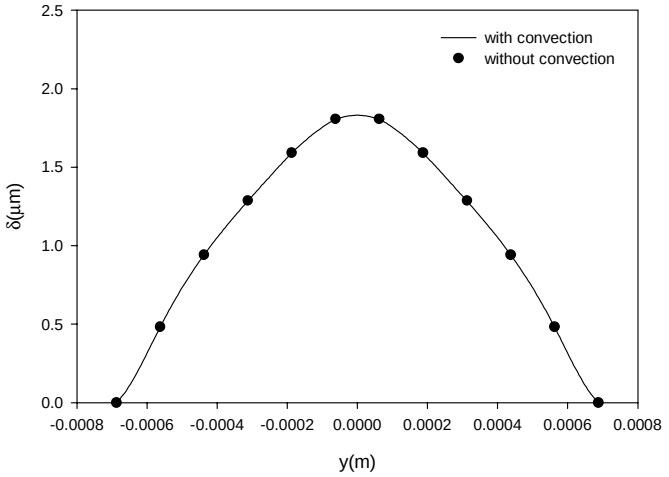

Fig. 4 Comparison of cross sectional area (P=300W, u_b=1.2mm/s)

The surface temperatures obtained by both methods are plotted in Fig. 2. The radius of the moving laser beam is $r_0=1.41\times10^{-4}$ m, which is very small in order to simulate the conduction in the substrate subject to a moving point heat source. It is seen that the overall agreement between the two solutions is very good except at the locations near x=0. This discrepancy of the two results is due to the nature of heat source modeled in analytical and numerical solution. The analytical result is that the temperature distribution is caused by an infinitesimal heat source at x=0, while the numerical temperature distribution result is caused by a finite size heat source. Considering the different models, the agreement between the numerical and analytical solutions is very good at all locations.

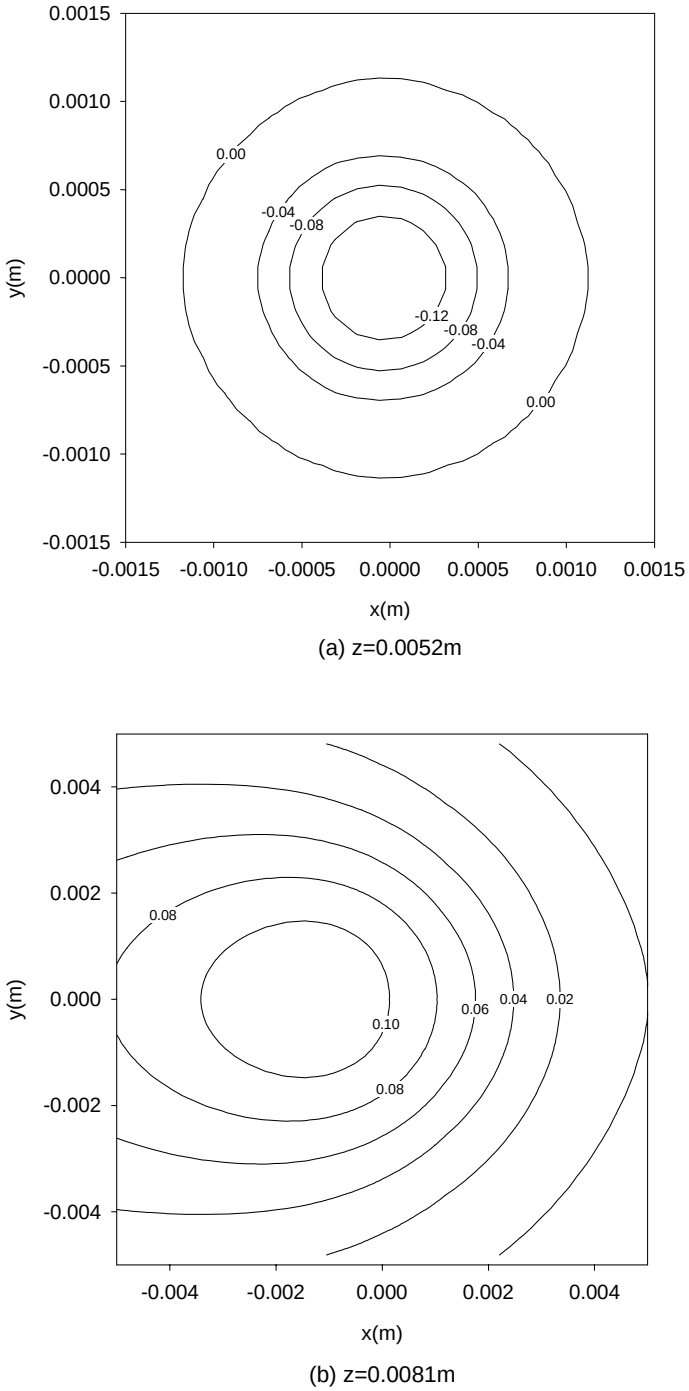

Fig. 5 Velocity component in z direction (P=300W, u_b=1.2mm/s)

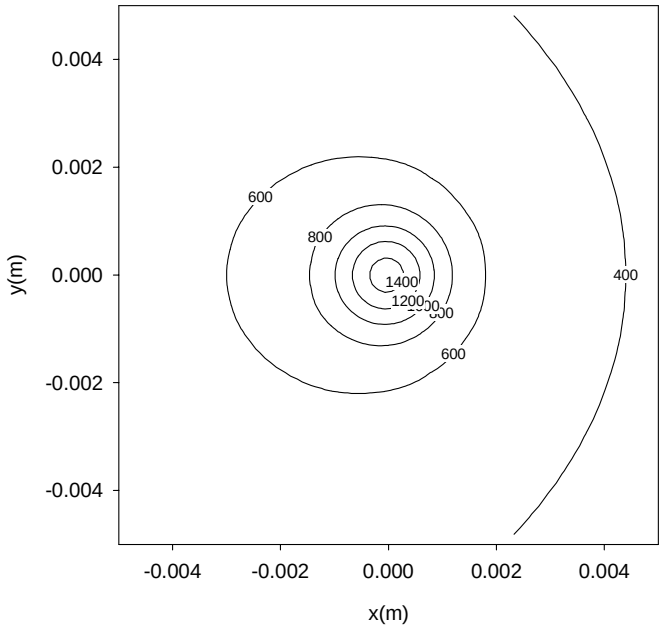

(a) with convection

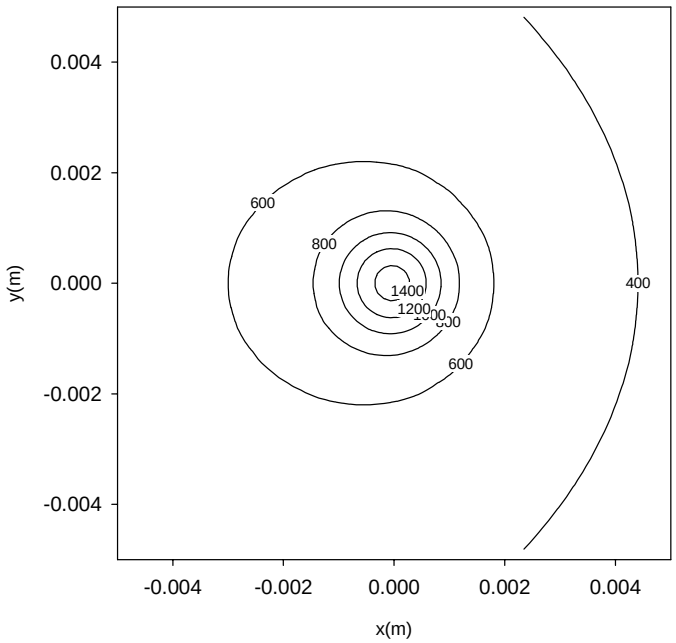

(b) without convection

Fig. 6 Comparison of substrate surface temperature (P=300W, u_b=1.2mm/s)

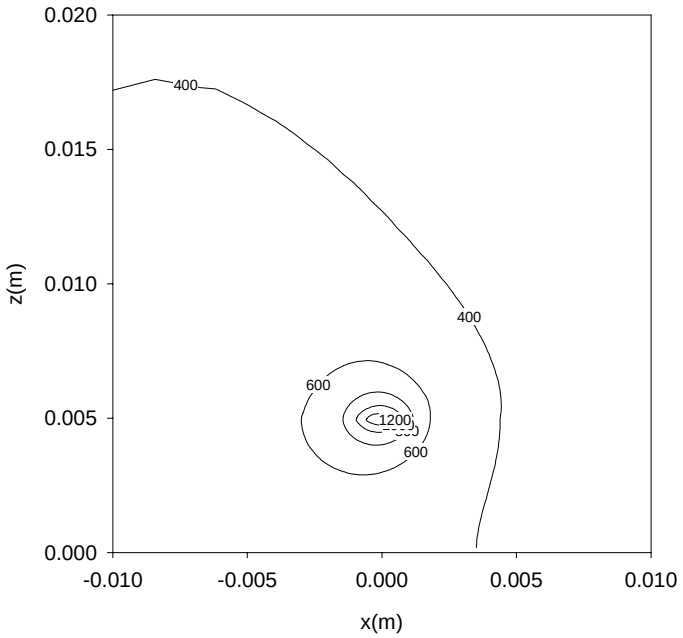

(a) with convection

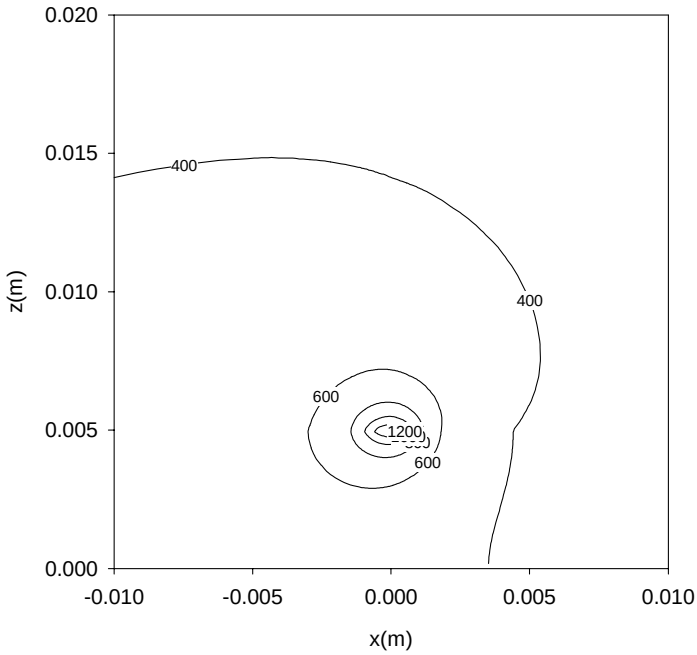

(b) without convection

Fig. 7 Temperature contour (P=300W, u_b=1.2mm/s, y=0)

The numerical simulations of the LCVD process are performed with parameters similar to those in Ref. [9]. The radius of the laser beam is very small compared with that of the chamber and therefore, the LCVD problem can be modeled as the LCVD on a substrate with infinite finite length and width. The validity of this assumption, of course, depends on the actual size of the substrate. On the other hand, it allows us to obtain quasi-steady state solution and parametric study can be performed. The computational domain (the size of the chamber) used in this paper is $0.5\times0.5\times0.125$ m³ (x×y×z) to ensure that the effect of the computational domain on the temperature distribution and deposited film can be eliminated. The thickness of the substrate is 5 mm and the bottom of the substrate is assumed to be adiabatic. The radius of the laser beam, which is defined as the radius where the laser intensity is $1/e^2$ of the intensity at the center of the laser beam, is 1.0×10^{-3} m. The absorptivity of the laser beam at the substrate surface is taken to be 0.23 [7,17]. The activation energy of the chemical reaction is taken to be E=51.02 KJ/mol. The constant K_0, as defined in eq. (8a), is 8.4m/s. Chemical reaction heat, ΔH_R, as determined by using JANAF thermochemical tables [18], is 5.379×10^6 J/kg.

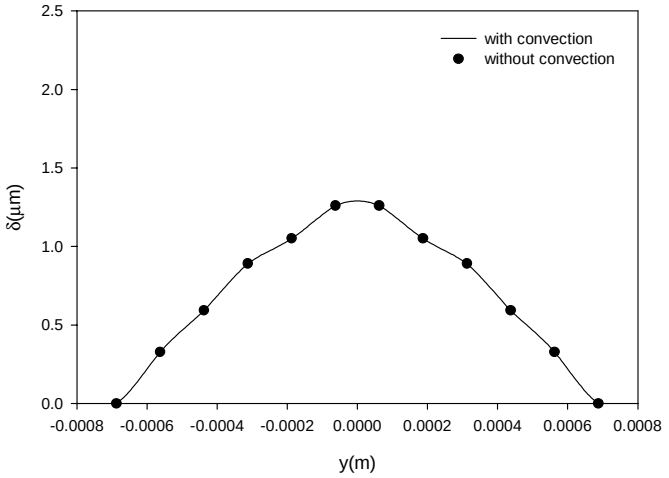

Fig. 8 Comparison of cross sectional area (P=300W, u_b=1.6mm/s)

Figure 3 shows the shape of the deposited TiN film obtained by using a laser power of 300W and scanning velocity of 1.2mm/s. The total pressure in the chamber is 207 torr and the partial pressure of Titanium Chloride is maintained at 7 torr. The partial pressures of N_2 and H_2 are the same. It can be seen that the cross sectional area is not functions of x at locations in the wake of the laser beam. The growth of the thin film only occurs in the spot directly under laser beam irradiation. Figure 4 shows the comparison of the cross sectional area of the thin film formed by LCVD process. The cross-sectional areas obtained by models with and without convection are plotted. The deposited TiN film thicknesses obtained by models with and without convection are very close: the difference at the top of the thin film laser beam is only 0.09%. Figure 5 shows the velocity components in z direction at different height. Since chemical reaction takes place on the hot spot of substrate under laser irradiation, gases flow toward the hot spot due to consumption of $TiCl_4$. Therefore, the velocity component in z direction is negative at z=0.0052m, which is only 0.2mm above the top of the substrate surface. The contour of w at this height is nearly circular even the entire the system moves with a velocity of $-u_b$. At another height, z=0.0081m, the velocity component in z direction near the center of the laser beam is positive due to natural convection. The region affected by natural convection at higher location is also significantly larger than that at the lower location. The location with high velocity is shifted toward the negative x direction since the entire system moves with $-u_b$ in the moving coordinate system. Figure 6 illustrates the surface temperature contour on the top of the substrate. The isotherms on the top of the substrate for the models with and without natural convection are almost the same, which means that natural convection have very little effect on the surface temperature of the substrate. As the result, the effect of natural convection on the cross sectional area of the deposited film is negligibly small as indicated in Fig. 3. The temperature contour at y=0 is shown in Fig. 7. It is seen that the isotherms for T>600K and for the cases with and without convection are almost the same. On the other hand, the isotherms for T=400K are significantly different for cases with and without convection.

Figure 8 shows predicted deposited TiN film thickness with the same laser power (P=300W) but a fast scanning velocity of u_b=1.6mm/s. The maximum thickness of the deposited thin film is 30% smaller than that for u_b=1.2mm/s because the time for any giving spot exposed under laser irradiation is shorter. Similar to the case of u_b=1.2mm/s, the results obtained by models with and without convection are very close to each other. The velocity components in z direction at different heights are shown in Fig. 9. The contours are similar to the case of u_b=1.2mm/s but the contours for both heights are slightly shifted to the negative x direction due to a higher scanning velocity is used. Figure 7 shows the temperature contour at y=0, which is qualitively similar to that at the lower scanning velocity. However, the entire contours are shifted to the left and the region affected by the laser beam is smaller than that at the lower scanning velocity.

The comparison of cross sectional areas obtained by models with and without natural convection is shown in Fig. 11. The scanning velocity is same as that in the case of Fig. 4, but the laser power is increased to 360 W. The deposited film is much higher and wider than that at lower power of 300 W. Another phenomenon that can be observed is that there is a groove exists on the top of the deposited film because the larger laser power makes the top surface temperature of the substrate in some points exceeds the critical temperature, above which the product of the chemical reaction can not be fully stuck on

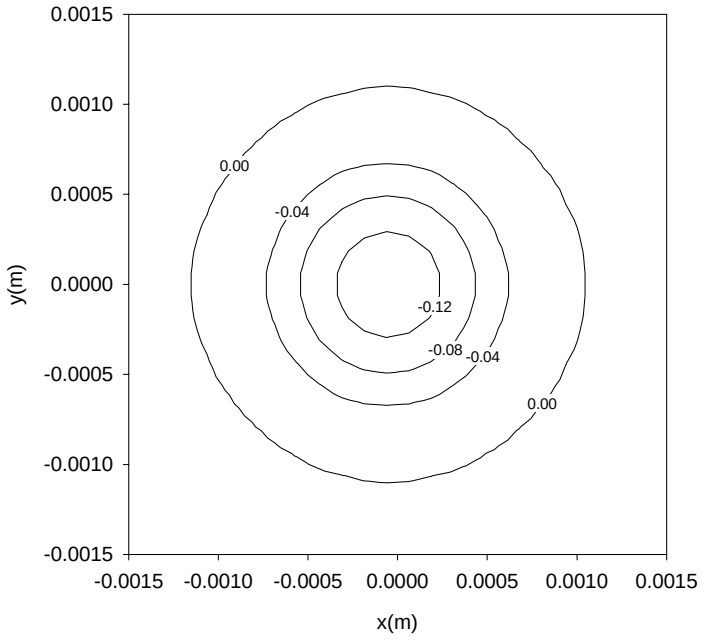

(a) z=0.0052m

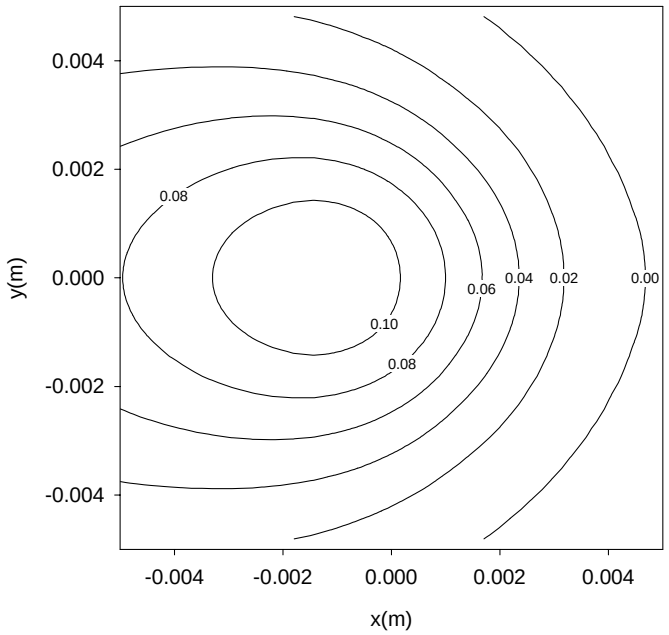

(b) z=0.0081m

Fig. 9 Velocity component in z direction (P=300W, u_b=1.6mm/s)

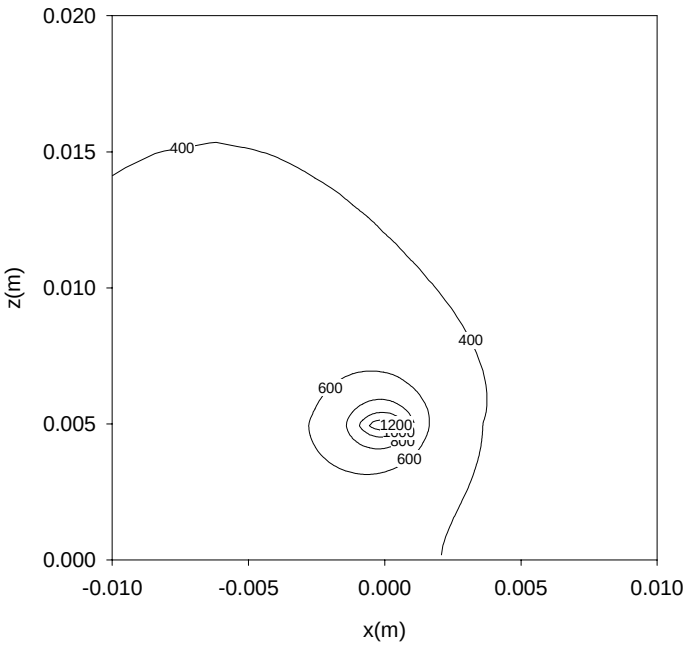

(a) with convection

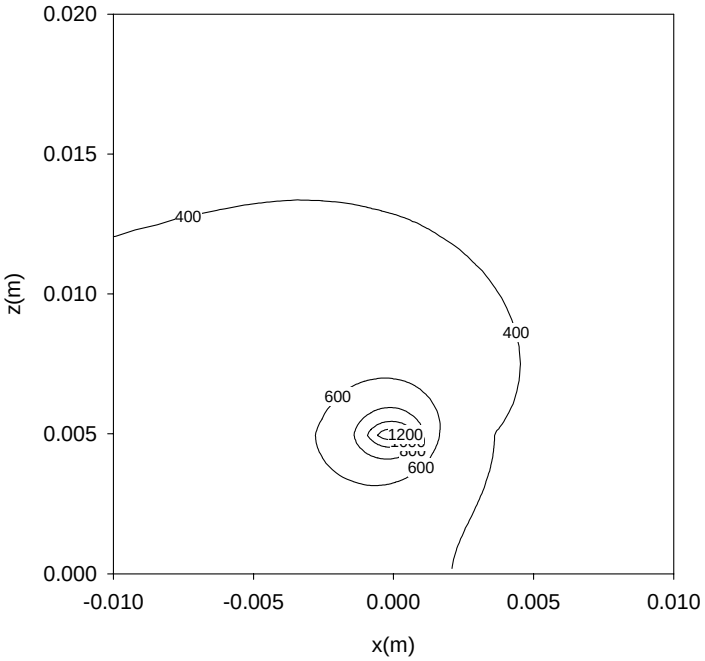

(b) without convection

Fig. 10 Temperature contour (P=300W, u_b=1.6mm/s, y=0)

the substrate surface [19]. In lieu of formation of the volcano-like film in the case of stationary laser beam [9], a groove is formed on the top of the deposited film. The groove is deeper for the case without convection and the effect of natural convection makes the groove shallower. This effect of natural convection on the shape of the deposited film can be explained by the fact that natural convection makes the surface temperature more uniform. However, the overall cross sectional areas for the cases with and without natural convection are almost not affected by natural convection. The velocity components in z direction at different heights for P=360W and u_b=1.2mm/s are shown in Fig. 12. The velocity at z=0.0052m for the case of P=360W is doubled compared to that of P=300W because more gases are consumed due to chemical reaction. The zone affected by laser beam is also significantly larger for higher laser power. The increase of the velocity at z=0.0081m by increasing laser power is not as much as that at z=0.0052m. For larger laser power, the region affected by natural convection is larger and it shifted to the negative x direction. The comparison of the temperature contour at y=0 is shown in Fig. 13. The effect of natural convection on the temperature contour is more significant for the case of larger laser power.

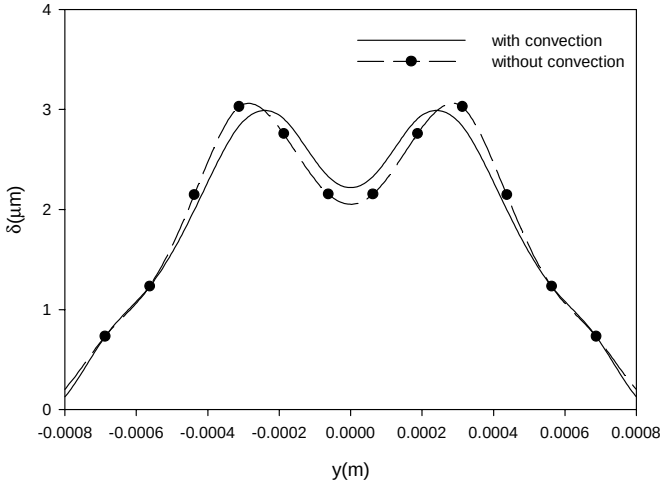

Fig. 11 Comparison of cross sectional area (P=360W, u_b=1.2mm/s)

Figure 14 shows predicted deposited TiN film thickness with a fast scanning speed of u_b=1.6mm/s but the laser power remains at 360W. It can be seen that the thickness of the deposited thin film is significantly reduced and the top of the film is nearly flat, which is very desirable for SALD process. Natural convection still plays an important role on the shape of the cross sectional area. Fig. 15 shows the velocity components in z direction at different heights. The shapes of the contours are very similar to the case of u_b=1.2mm/s except the contours for both heights are slightly shifted to the negative x direction due to higher scanning velocity. Figure 16 shows the temperature contour at y=0, which indicated that the entire contours are shifted to the left and the region affected by the laser beam is smaller than that at the lower scanning velocity.

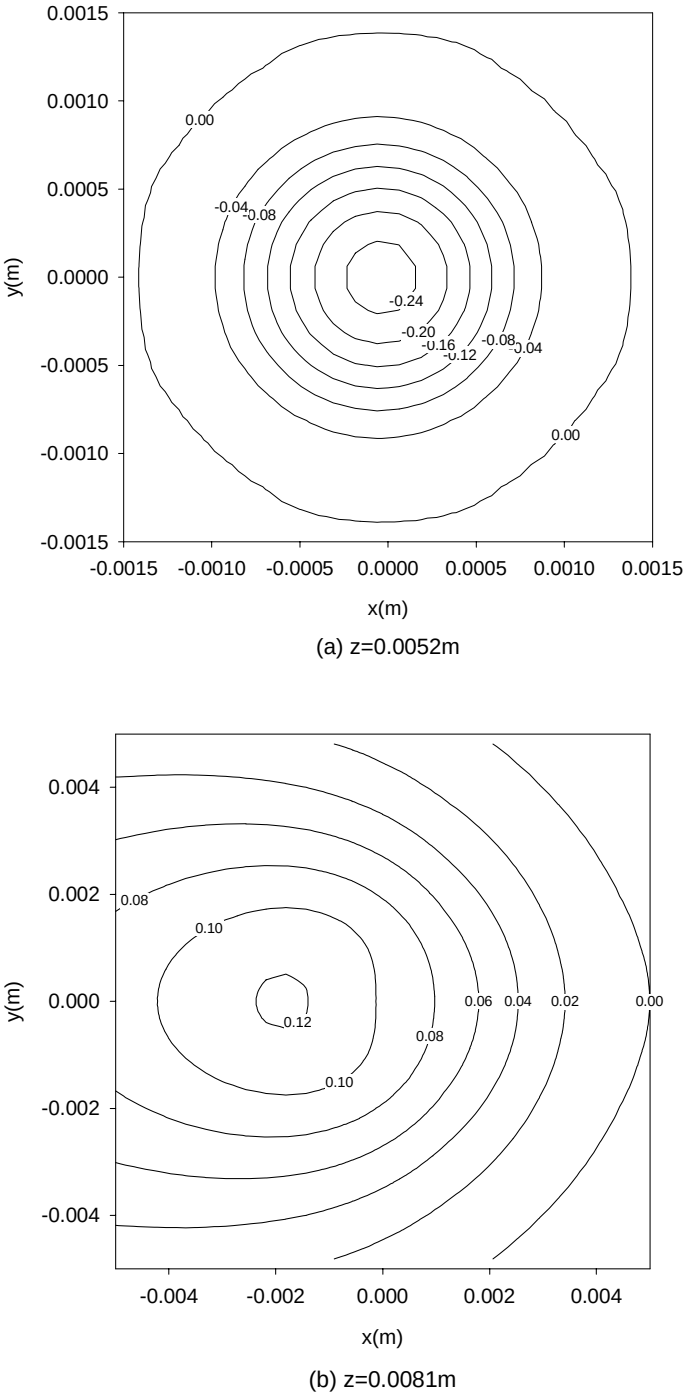

Fig. 12 Velocity component in z direction (P=360W, u_b=1.2mm/s)

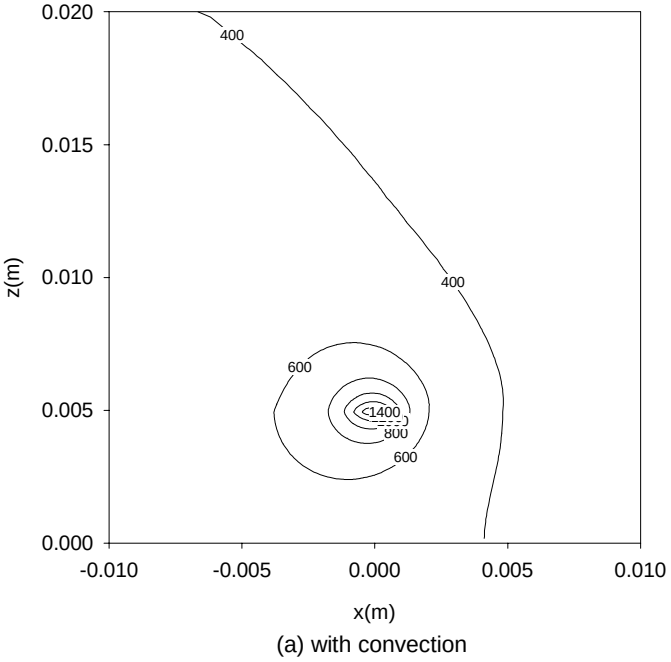

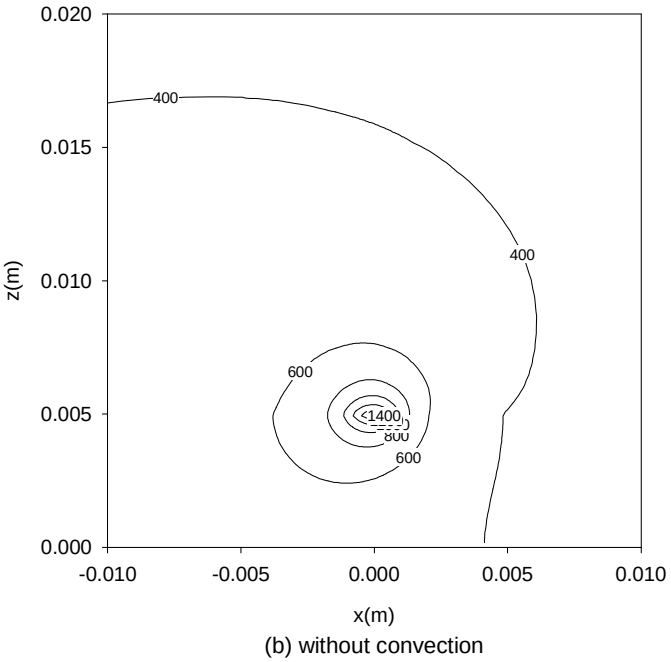

Fig. 13 Temperature contour (P=360W, u_b=1.2mm/s, y=0)

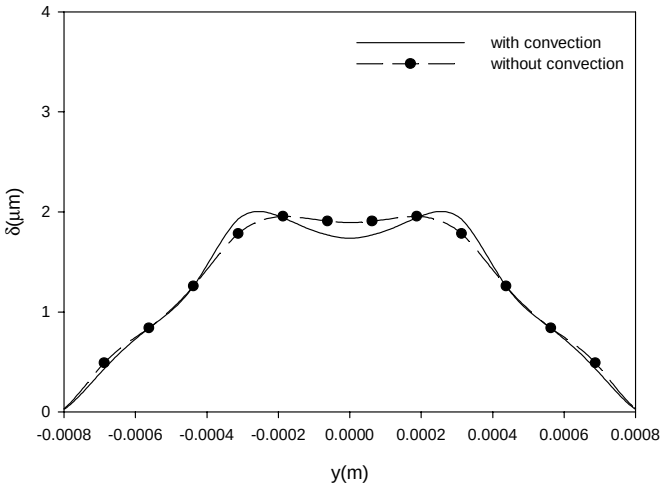

Fig. 14 Comparison of cross sectional area (P=360W, u_b=1.6mm/s)

CONCLUSIONS

Quasi-steady state natural convection in the LCVD of TiN film on a substrate with moving laser beam is investigated numerically. The results show that the effect of natural convection on the shape of deposited film is negligible for the laser power of P=300W. When the laser power is increased to 360W, a groove is observed on top of the thin film and the effect of natural convection on the shape of the cross sectional area becomes important. The velocity components in z direction are negative at the locations near the substrate surface under laser irradiation because chemical reaction takes place on the surface consumed $TiCl_4$. At the locations far from the substrate surface, the velocity component in z direction near the center of the laser beam becomes positive due to natural convection driven by the temperature gradient in the gases. The effect of natural convection have very little effect on the temperatures near the hot spot under laser irradiation but have significant effect on the size of the regions affected by the laser heating.

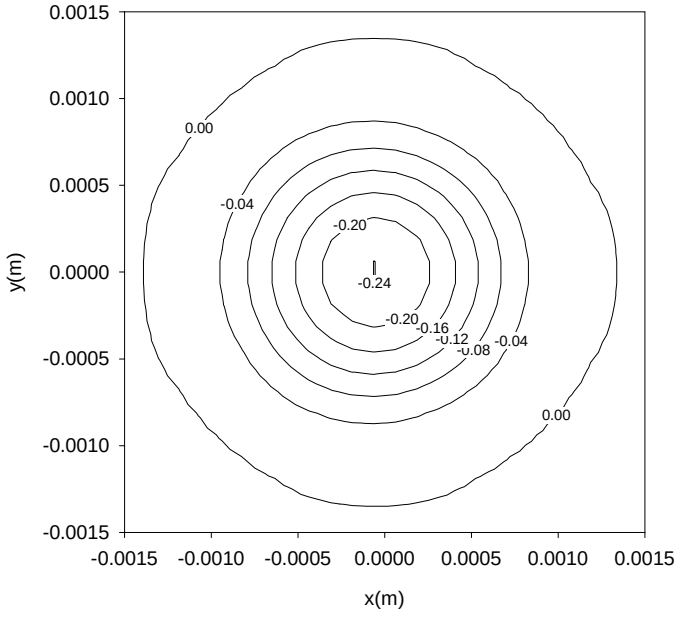

(a) z=0.0052m

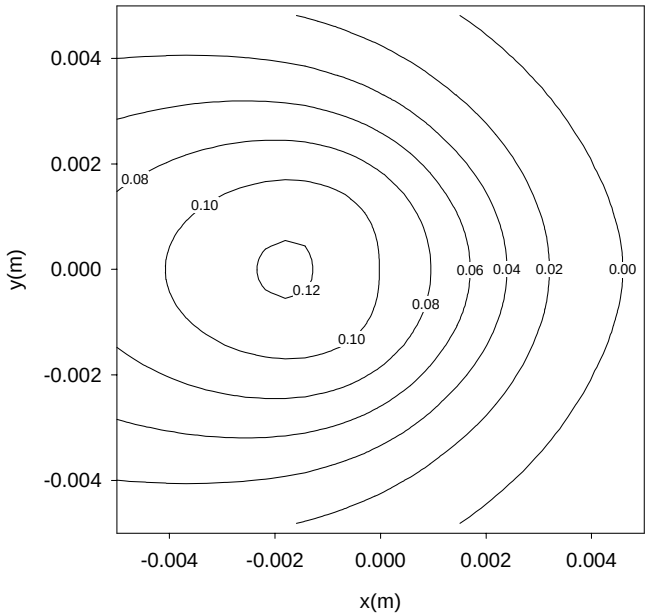

(b) z=0.0081m

Fig. 15 Velocity component in z direction (P=360W, u_b=1.6mm/s)

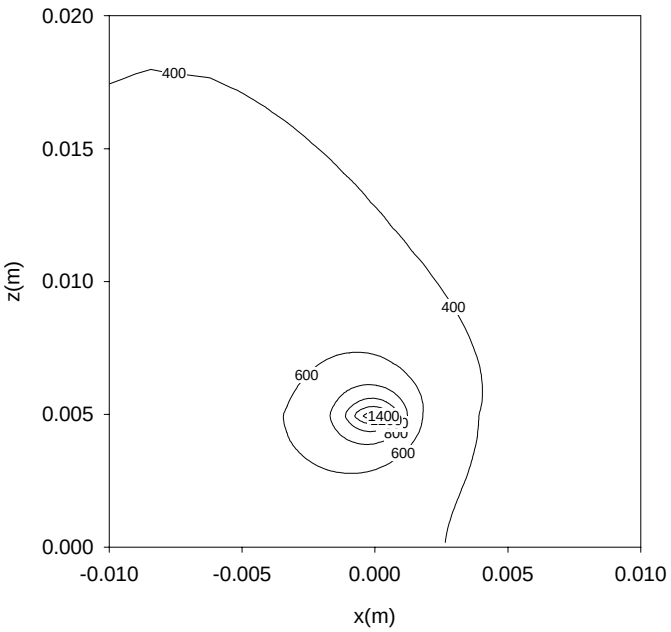

(a) with convection

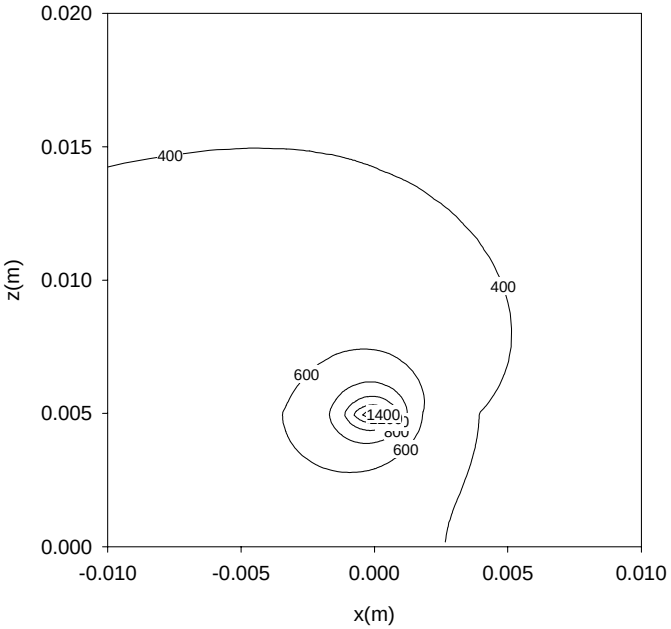

(b) without convection

Fig. 16 Temperature contour (P=360W, u_b=1.6mm/s, y=0)

REFERENCES

1. J.G. Conley and H.L. Marcus, Rapid Prototyping and Solid Freeform Fabrication, ASME J. of Manufacturing Science and Engineering 119 (1997), 811-816.
2. H.L. Marcus, G. Zong and P.K. Subramanian, Residual Stresses in Laser Processed Solid Freeform Fabrication, in Residual Stresses in Composites: Measurement, Modeling and Effect on Thermomechanical Properties, Edited by E.V. Barrera and I.Dutta, TMS, 1993.
3. K.J. Jakubenas, B. Birmingham, S, Harission, J. Croker, M.S. Shaarawi, J.V. Tomkins, J. Sanchez, and H. Marcus, Recent Advances in SALD and SALDVI, Procs. of 7th International Conference on Rapid Prototyping, San Francisco, CA, March, 31- April 3, 1997.
4. K.J. Jakubenas, Y.L. Lee, M.S. Shaarawi, H. Marcus and J.M. Sanchez, Selective Area Laser Deposition of Titanium Oxide, Rapid Prototyping Journal, Vol. 3, pp. 66-70, 1997.
5. S. Harrison and H.L. Marcus, Gas-phase Selective Laser Deposition (SALD) Joining of SiC, Materials and Design, Vol. 20, pp. 147-152, 1999.
6. R.L. Marhajan, Transport Phenomena in Chemical Vapor-Deposition Systems, Advances in Heat Transfer, Academic Press, San Diego, 1996.
7. J. Mazumder and A. Kar, Theory and Application of Laser Chemical Vapor Deposition, Plenum Publishing Co., New York, 1995.
8. Y. Jacquot, G.-S. Zong and H.L. Marcus, Modeling of Selective Laser Deposition for Solid Freeform Fabrication, Proceedings of Solid Freeform Fabrication Symposium 1995, 74-82.
9. Y. Zhang and A. Faghri, Thermal Modeling of Selective Area Laser Deposition of Titanium Nitride on a Finite Slab with Stationary and Moving Laser Beams, Int. J. Heat Mass Transfer, 43(2000), 3835-3846.
10. Y.L. Lee, J.V. Tompkins, J.M. Sanchez and H.L. Marcus, Deposition Rate of Silicon Carbide by Selected Area Laser Deposition, Proceedings of Solid Freeform Fabrication Symposium 1995, 433-439.
11. O. Manca, B. Morrone and V. Naso, Quasi-Steady-State Three-Dimensional Temperature Distribution induced by a Moving Circular Gaussian Heat Source in a Finite Depth Solid, Int. J. Heat Mass Transfer, Vol. 38, pp. 1305-1315.
12. R.B. Bird, W.E. Stewart and E.N. Lightfoot, Transport Phenomena, John Wiley & Sons, New York, 1960.
13. S.V. Patankar, Numerical Heat Transfer and Fluid Flow, Hemisphere, Washington, DC, 1980.
14. J.P. Van Doormaal and G.D. Raithby, Enhancements of the Simple Method For Predicting Incompressible Fluid Flows, Numerical Heat Transfer, Vol. 7, pp. 147-163, 1984.
15. M. Yang and W.Q. Tao, Numerical Study of Natural Convection Heat Transfer in a Cylindrical Envelop with Internal Concentric Slotted Hollow Cylinder, Numerical Heat Transfer, Part A, Vol. 22, pp. 289-305, 1992.
16. Carslaw, H.S., and Jaeger, J.C., Conduction of Heat in Solids, Clarendon, Oxford, 1959.
17. A. Kar and J. Mazumder, Three-Dimensional Transient Thermal Analysis for Laser Chemical Vapor Deposition on Uniformly Moving Finite Slabs, J. of Applied Physics, 65(1989), 2923-2934.
18. W.M. Chase, JANAF Thermochemical Tables, 3rd Edition, J. Phys. Chem. Ref. Data 14 (1986), Suppl. 1.
19. O. Conde, A. Kar and J. Mazumder, Laser Chemical Vapor Deposition of TiN Dot: A Comparison of Theoretical and Experimental Results, J. Applied Physics 72 (1992), 754-761.